NATIONAL ADVISORY COMMITTEE FOR AERONAUTICS

TECHNICAL NOTE 3969

A THEORETICAL STUDY OF THE EFFECT OF UPSTREAM TRANSPIRATION COOLING ON THE HEAT-TRANSFER AND SKIN-FRICTION CHARACTERISTICS OF A COMPRESSIBLE, LAMINAR BOUNDARY LAYER

By Morris W. Rubesin and Mamoru Inouye

Ames Aeronautical Laboratory
Moffett Field, Calif.

NACA

Washington
May 1957

F

NATIONAL ADVISORY COMMITTEE FOR AERONAUTI(

TECHNICAL NOTE 3969

A THEORETICAL STUDY OF THE EFFECT OF UPSTREAM TRANSPIRATION COOLING ON THE HEAT-TRANSFER AND SKIN-FRICTION CHARACTERISTICS OF A COMPRESSIBLE, LAMINAR BOUNDARY LAYER

By Morris W. Rubesin and Mamoru Inouye

SUMMARY

An analysis is presented which predicts the skin-friction and heat-transfer characteristics of a compressible, laminar boundary layer on a solid flat plate preceded by a porous section that is transpiration cooled. The analysis is restricted to a Prandtl number of unity and linear variation of viscosity with temperature.

The local skin friction has been found to have a low value in the region of transpiration cooling and then to increase until it approaches the value for a completely nonporous surface asymptotically. The initial increase in local skin friction is rapid as half of the ultimate increase occurs in a distance beyond the porous region that is about 20 percent of the length of the porous region for all rates of injection. When the total coolant flow rate is kept constant and the porous length is varied, it is found that the average skin friction on a partially porous plate is slightly lower than that on a fully porous plate.

The local heat transfer behaves in a manner similar to that of the local skin friction. It is found, in an example, that the temperature at the end of a partially porous plate could be maintained at about the same temperature as a fully porous plate by doubling the total rate of coolant flow.

INTRODUCTION

For flight at high speeds, aerodynamic heating often requires the cooling of aircraft in order to maintain tolerable surface temperatures. Of the various cooling techniques available, transpiration cooling systems are usually effective for this application, as is shown in reference 1. This results because the geometry of the porous surface provides for excellent heat exchange between the coolant and the surface, and the boundary layer on the surface is altered so as to reduce significantly the skin friction and the heat transfer to the surface.

The attractiveness of transpiration cooling of large surfaces is reduced by the introduction of structural problems. It is difficult to manufacture large porous surfaces and to support them in use because of their inherent weakness. To take advantage of transpiration cooling and also to alleviate the structural problems, the use of partially porous surfaces offers possibilities. In this scheme, the most critical regions from an aerodynamic heating standpoint could be transpiration cooled, and the downstream regions protected by the film of coolant that is introduced into the boundary layer.

It is the purpose of this investigation, therefore, to examine theoretically the magnitude of protection offered the downstream nonporous regions by the film cooling process. The present analysis is restricted to consideration of a compressible, laminar boundary layer on a semi-infinite flat plate with air as the coolant. The flat plate is divided into two regions: an upstream region of finite length which is porous and transpiration cooled, and a downstream region which is nonporous and is protected by the upstream cooling process.

SYMBOLS

$a_n(x)$, a	dimensionless coefficients in assumed velocity profile polynomial (A19) (The subscript is dropped for $n = 1$.)
a_B	constant value of a for no transpiration or Blasius solution
C	constant of proportionality between absolute viscosity and absolute temperature defined in equation (A6)
c_f	local skin-friction coefficient, $\frac{\tau_s}{\frac{1}{2}\rho_\infty u_\infty^2}$
c_p	specific heat at constant pressure
D_o	constant, $\frac{R_{\delta_o}^2}{R_{x_o}}$
$f(\eta)$	dimensionless stream function used in reference 2 such that $f'(\eta) = 2\frac{u}{u_\infty}$
$f(0) = F$	dimensionless number which is proportional to the mass flow of transpiration cooling (See eq. 5.)
k	thermal conductivity of fluid
L	length of plate
Pr	Prandtl number, $\frac{c_p\mu}{k}$

p	pressure
q	heat-transfer rate per unit area
R	gas constant
R_x	Reynolds number, based on distance x, $\frac{\rho_\infty u_\infty x}{C\mu_\infty}$
R_δ, R_{x_o}, R_{δ_o}, R_L	Reynolds numbers based on δ, x_o, δ_o, L
$s(x)$	slope of velocity profile at surface, $\left(\frac{\partial u}{\partial y}\right)_{y=o}$
T	absolute temperature
u	velocity component parallel to surface
v	velocity component normal to surface
w	total coolant flow rate
x	transformed coordinate along surface defined in equation (A9)
x'	physical coordinate along surface
y	transformed coordinate normal to surface defined in equation (A9)
y'	physical coordinate normal to surface
Γ	gamma function
δ	boundary-layer thickness in transformed coordinates
δ^+	dimensionless boundary-layer thickness, $\frac{\delta}{\delta_o} = \frac{R_\delta}{R_{\delta_o}}$
η	similarity parameter used in reference 2, $\frac{y}{2}\sqrt{\frac{u_\infty}{\nu_\infty xC}}$
η_δ	value of η corresponding to the edge of the boundary layer
θ	dimensionless temperature function defined in equation (A59), $\frac{T-T_s}{T_\infty-T_s}$
μ	absolute viscosity
ν	kinematic viscosity

ξ dimensionless length along surface, $\frac{x}{x_o} = \frac{R_x}{R_{x_o}}$

ρ density

σ dimensionless slope of velocity profile at surface,

$$\frac{a}{\delta^+} = \frac{\delta_o}{u_\infty} s(x)$$

τ_s shear stress at surface

$\varphi(\xi)$ function defined in equations (A83)

Subscripts

c transpiration cooled surface

cl coolant

s surface

t stagnation conditions

∞ free stream

o conditions at end of porous region

Superscripts

' quantities related to original physical coordinates

$(\bar{\ })$ average

ANALYSIS

Conditions and Assumptions

The analysis is performed for a compressible, laminar boundary layer on a nonporous flat plate behind a porous region which is transpiration cooled. The geometry is shown in figure 1. The analysis can employ any of existing solutions (such as refs. 2, 3, and 4) for the transpiration cooled region, and use their results at $x' = x_o'$ to begin the present analysis. For convenience, the solution (refs. 2 and 3) containing the following conditions is employed:

1. The coolant is the same as the boundary-layer fluid.

2. The velocity of the coolant normal to the surface is inversely proportional to the square root of the distance from the leading edge.

3. The porous surface temperature is constant.

In addition, the following assumptions concerning the boundary-layer fluid are made:

1. Prandtl number is unity.

2. Specific heat at constant pressure is constant.

3. The fluid behaves as a perfect gas; $p = \rho RT$.

4. The absolute viscosity varies linearly with the absolute temperature.

Summary of Analysis

The mathematical details of the analysis are included in Appendix A, and only a summary is presented here.

Transformation of basic equations.- The analysis is begun with the basic equations of continuity, momentum, and energy for a compressible, laminar boundary layer with no pressure gradient. By use of the Stewartson transformation (ref. 5) in which the physical coordinate normal to the surface is modified to take into account the compressibility, the basic equations are reduced to the equations for an equivalent, incompressible flow. This transformation not only simplifies the equations, but together with the previous assumptions concerning the fluid, permits solution of the momentum equation independently of the energy equation.

Solution of momentum equation for skin friction.- To begin the present solution, it is necessary to start with velocity distributions that match those of the boundary layer at the end of the porous region where transpiration cooling ceases. Because these velocity distributions change from those characteristic of transpiration cooling to those characteristic of flow along a solid surface far downstream along the plate, similarity of profiles cannot be expected, and an exact solution is not simple to obtain. Therefore, the momentum integral method of solution was chosen.

A convenient and fairly accurate velocity distribution can be found using the following procedure. The boundary-layer velocity profile for use in the momentum integral equation is approximated by a seventh-degree polynomial in terms of y/δ,

$$\frac{u}{u_\infty} = a\left(\frac{y}{\delta}\right) + a_2\left(\frac{y}{\delta}\right)^2 + a_3\left(\frac{y}{\delta}\right)^3 + a_4\left(\frac{y}{\delta}\right)^4 + a_5\left(\frac{y}{\delta}\right)^5 + a_6\left(\frac{y}{\delta}\right)^6 + a_7\left(\frac{y}{\delta}\right)^7 \qquad (1)$$

where y is the transformed distance normal to the surface and δ is the transformed boundary-layer thickness. The coefficient of the first term, a, is a measure of the shear stress or the slope of the velocity profile at the surface. The seven unknown coefficients of the polynomial and the boundary-layer thickness make a total of eight unknowns to be determined. In addition to the momentum integral equation, seven other equations are necessary in order to solve the problem. These equations are obtained by imposing seven boundary conditions on the velocity profile. Four of the conditions are imposed at the outer edge of the boundary layer and three at the surface. To insure that the local velocity in the boundary layer approaches the free-stream velocity smoothly, it is required that for $y = \delta$

$$\left.\begin{aligned} & u = u_\infty \\ & \frac{\partial u}{\partial y} = \frac{\partial^2 u}{\partial y^2} = \frac{\partial^3 u}{\partial y^3} = 0 \end{aligned}\right\} \tag{2}$$

To insure that the velocity profile has the correct slope and curvature at the surface, the velocity distribution and the boundary conditions $u = v = 0$ are inserted into the basic momentum equation and its derivatives with respect to y. This yields for $y = 0$ (see eqs. (A16), (A24), and (A25))

$$\left.\begin{aligned} & \frac{\partial^2 u}{\partial y^2} = \frac{\partial^3 u}{\partial y^3} = 0 \\ & \frac{\partial u}{\partial y} \frac{\partial}{\partial x}\left(\frac{\partial u}{\partial y}\right) = C\nu_\infty \frac{\partial^4 u}{\partial y^4} \end{aligned}\right\} \tag{3}$$

These boundary conditions permit the evaluation of the unknown coefficients of the polynomial in terms of the first coefficient a, and lead to an ordinary differential equation relating a, δ, and x. This equation and the momentum integral equation are solved simultaneously along the plate.

Before the differential equations can be solved, initial conditions for these differential equations must be determined. The initial conditions for the present solution are obtained by matching the seventh-degree polynomial velocity profile to the exact velocity distribution at the end of transpiration cooling. This is accomplished by equating the slopes at the wall and the boundary-layer thicknesses of the two velocity distributions. A problem arises in the definition of the boundary-layer thickness. In the exact solution, the local velocity in the boundary layer approaches the free-stream velocity asymptotically, whereas with a polynomial solution the local velocity equals the free-stream velocity at a finite distance from the surface. In this analysis, the boundary-layer thickness for the exact velocity distribution is chosen as the point where $u/u_\infty = 0.9976$, and the reason for this choice is in Appendix A.

With these initial conditions, the system of two simultaneous ordinary differential equations was integrated numerically yielding δ and a as functions of x. The local skin-friction coefficient was then calculated directly from these results.

Solution of energy equation.- Normally, the surface temperature of the nonporous region will vary and differ from the constant surface temperature of the transpiration cooled region. Hence, the solution of the energy equation must account for surface temperature variations. A convenient method of analysis is to separate the solution of the energy equation into two parts. First, a solution of the complete inhomogeneous energy equation is found for the condition that the porous and nonporous regions are at the same constant temperature. Then solutions of the homogeneous portion of the energy equation are found and added to satisfy the surface temperature boundary conditions. This addition of solutions is permissible because the energy equation is linear in temperature.

The inhomogeneous energy equation can be expressed in terms of total energy such that it has the same form as the momentum equation (since $Pr = 1$). Then, for the case of constant surface temperature, the boundary-layer temperature distribution can be expressed in terms of the velocity distribution, which has been solved previously.

Initially, the homogeneous portion of the energy equation is solved for the condition of a single surface temperature discontinuity behind the transpiration cooled region. In order to obtain a solution, the boundary-layer velocity profile is replaced by a linear profile having the correct slope at the surface as determined previously in the solution of the momentum equation. Then the temperature distribution in the boundary layer can be solved for in terms of a single similarity parameter, ζ.

The general solution of the energy equation, which takes into account arbitrary surface temperature variations, is obtained by adding the solution for the inhomogeneous energy equation to as many solutions of the homogeneous equation as required to satisfy the surface temperature boundary condition. For an arbitrary surface temperature distribution, the summation of the solutions of the homogeneous energy equation can be expressed as an integral. Hence, the general solution of the energy equation yields the temperature distribution in the boundary layer for an arbitrary surface temperature distribution.

The heat-transfer rate at the surface is obtained by differentiating the temperature distribution with respect to y'. If the surface temperature is given, the heat transfer can be determined. For the case of a constant surface temperature, the Reynolds analogy is applicable, and the local heat transfer is directly related to the local skin friction.

Thus far, it has been assumed that the surface temperature distribution is given as a boundary condition. In many cases, however, the heat transfer at the wall is given as a boundary condition, and the surface temperature distribution is desired. This problem is solved by using an integral equation based on the equation for the heat-transfer rate. In particular, the surface temperature distribution was solved numerically for the condition that the nonporous surface is insulated.

Results of Analysis

The results of the analysis are summarized in the following equations.

The local skin friction is given by

$$\frac{c_f}{2} = \frac{1}{R_{\delta_o}} \frac{a}{\delta^+} = \frac{1}{R_{\delta_o}} \sigma(\xi) \tag{4}$$

where

$$\xi = \frac{x}{x_o}$$

Note that both $\sigma(1)$ and R_{δ_o} are dependent on the transpiration coolant rate in the porous region and the Reynolds number of the porous region. For example, when the local blowing rate is expressed by $f(0) = F$ where

$$f(0) = -2 \frac{\rho_s v_s}{\rho_\infty u_\infty} \sqrt{R_x} = -\frac{\overline{\rho_s v_s}}{\rho_\infty u_\infty} \sqrt{R_x} \tag{5}$$

then

$$R_{\delta_o} = \sqrt{D_o(F) R_{x_o}} \tag{6}$$

$$\sigma(1) = \sigma(F) \tag{7}$$

Note that $\overline{\rho_s v_s} = 2\rho_s v_s$ because v_s varies inversely as $\sqrt{x}$. For convenience $D_o(F)$ and $\sigma(F)$ are tabulated as functions of $F = f(0)$ in table I. For $\xi > 1$ or $x > x_o$ a plot of $\sigma(\xi)$ for each $f(0)$ is given in figure 2.

If the surface temperature distribution is given, the local heat-transfer rate at the wall for $x > x_o$ is found from

$$q_s(\xi) = -\frac{\rho_\infty u_\infty c_p}{R\delta_o}\sqrt{\sigma(\xi)}\left\{(T_t-T_c)\sqrt{\sigma(\xi)} - 0.538 D_o^{1/3}\int_1^\xi \frac{\frac{dT_s(\xi_1)}{d\xi_1}\,d\xi_1}{[\varphi(\xi)-\varphi(\xi_1)]^{1/3}}\right\} \tag{8}$$

where

$$\varphi(\xi) = \int_1^\xi \sqrt{\sigma(\xi)}\,d\xi \tag{9}$$

The function $\varphi(\xi)$ is presented in figure 3 for various $f(0)$.

If the heat-transfer rate at the surface is given, the surface temperature distribution can be determined from

$$T_s(\xi)-T_c = \frac{0.512}{D_o^{1/3}}\int_1^\xi \frac{\frac{R\delta_o q_s(\xi_1)}{\rho_\infty u_\infty c_p} + (T_t-T_c)\sigma(\xi_1)}{[\varphi(\xi)-\varphi(\xi_1)]^{2/3}}\,d\xi_1 \tag{10}$$

RESULTS AND DISCUSSION

Comparison of Polynomial and Exact Velocity Distribution

As explained in the analysis, at the start of the nonporous region, the seventh-degree velocity profile must match the exact transpiration cooling profile as given in reference 2. To do this, the polynomial velocity was made to have the same slope at the surface and to have the same boundary-layer thickness as the exact velocity profile. A comparison of the two entire profiles is shown in figure 4 for three transpiration cooling rates where the absolute magnitude of $f(0)$ is proportional to the amount of transpiration cooling. The agreement between the respective profiles throughout the boundary layer is satisfactory. Because the Prandtl number is assumed to be unity, agreement of the velocity profiles implies an agreement of the corresponding temperature distributions.

Skin Friction

The effect of upstream surface transpiration cooling on the local skin friction is shown in figure 5. The abscissa is the ratio of the distance from the leading edge to the length of the porous region. The ordinate is the local skin-friction coefficient with upstream transpiration cooling divided by the local skin friction that would exist with no transpiration cooling. This figure was obtained from figure 2. For each transpiration cooling rate, the reduction of skin friction diminishes rapidly with downstream distance and approaches the no transpiration solution asymptotically. For example, continuous transpiration cooling of $f(0) = -0.50$ halves the skin friction. With a finite transpiration-cooled region, however, the skin friction rises to within 13 percent of the no transpiration value at $\xi = 2$ and to within 5 percent at $\xi = 6$. Similar effects are shown for the other transpiration coolant rates.

Heat Transfer

The effect of upstream surface transpiration cooling on the heat-transfer characteristics of the nonporous region was evaluated for two cases: the local heat transfer at the surface was determined if the surface temperature distribution was prescribed, and the surface temperature distribution was determined if the local heat transfer at the surface was prescribed.

The first case occurs when the surface temperature is constant over both the porous and nonporous regions. By Reynolds analogy, the effect of upstream surface transpiration cooling on the heat-transfer rate is the same as the effect on the skin friction shown in figure 5. For example, at $\xi = 2$ with $f(0) = -0.50$, the internal heat-transfer rate necessary to maintain a constant surface temperature is reduced 13 percent from the no transpiration value. Similar trends occur for the other transpiration coolant rates.

An example of the second case occurs when the nonporous region is insulated, or $q_s(\xi) = 0$. The resulting surface temperature distribution is shown as the ordinate in figure 6. The ordinate is written in dimensionless form employing the temperature of the cooled upstream region and the total temperature. It is observed for all coolant rates that the surface temperature of the nonporous region rises rapidly at first and ultimately approaches the recovery temperature asymptotically. The reduction in temperature due to the effect of injecting transpiration coolant into the boundary layer is not very large, however, as is noted when the rest of the curves are compared with the $f(0) = 0$ curve, which represents the temperature distribution caused by cooling the upstream section to T_c by some internal cooling system.

Practical Implications of Results

Figures 5 and 6 show how the skin friction and heat transfer behave on the nonporous section when air is transpired in the porous section. The parameter of these curves, $f(0)$, however, does not provide a satisfactory criterion for a practical evaluation of the usefulness of the cooling system under analysis. A more useful criterion is the total coolant flow rate. This permits comparison of various cooling systems on a corresponding weight basis.

For instance, it is interesting to know how the average skin friction on a plate changes as the proportion of the lengths of the porous and nonporous regions is varied, subject to the restriction that the total coolant flow rate be constant. Thus, as the porous region is reduced in length (actually area), the rate of coolant flow per unit area is increased. It is quite easy to calculate these effects using the results of figure 5. Thus, in figure 7, the ratio of the average skin friction on the plate to the corresponding average skin friction on an entirely solid plate is plotted as a function of the fractional length of the plate that is porous. The parameter of each curve is a dimensionless group containing a term representing the total coolant flow rate, w. Starting from the right side of the figure, it is noted that for a completely porous plate $(x_o/L = 1)$ there is a considerable reduction in skin friction for each coolant rate. As the fraction of porous surface is reduced, x_o/L becoming smaller, it is rather surprising that the reduction in average skin friction is even greater for each of the total coolant rates. Apparently, the greater reduction in the local skin-friction coefficient over the porous section of the plate due to the higher local coolant rate more than compensates for the rise in local skin friction experienced over the nonporous section as shown in figure 5. The line, at the left, represents an estimate of the lower bound of these results, because at a fixed total coolant rate the local coolant rate at points to the left of this dashed line becomes sufficiently large to separate the laminar boundary layer. The curves are drawn as far to the left as the information in figure 5 allows. It appears, therefore, that on the basis of average skin friction, no penalty results from restricting the transpiration cooled portion to a fraction of the total length of the plate when a given total amount of coolant is used.

In figures 8(a) and (b), there are shown the temperature distributions that result from using a fixed quantity of coolant flow with various lengths of porous regions. The ordinate represents the surface temperature expressed in terms of the recovery temperature, which for $Pr = 1$ is the total temperature, and the initial coolant temperature. It can be seen in figure 8(a) that for the amount of coolant used, a fully porous plate would result in a dimensionless surface temperature of about 0.66. The temperature distributions resulting from the plate being 0.5, 0.25, and 0.1 porous are indicated also. For these cases, the temperature of the porous regions is reduced markedly because of the high local rate of coolant flow. The reductions in the porous surface temperature, however, are not sufficient to lower the surface temperature over most of the rest of the surface down to the value of the fully porous case. It is significant that even at the end of the plate, in these examples, the surface temperature is well below the recovery temperature. As an example of these temperatures consider an aircraft flying at a Mach number of 5 under steady-state conditions, where the recovery temperature is about 1770° F. If cooled as in figure 8(a) with an entirely porous surface and a laminar boundary layer, the surface temperature would be about 1220° F for an initial coolant temperature of 150° F. With partial cooling, the maximum temperature at the trailing edge would be about 1460° F, or still about 300° F below the recovery temperature.

The effect of doubling the coolant flow rate is shown in figure 8(b). For the fully porous case the dimensionless surface temperature becomes about 0.4. The only partially porous case shown is where the plate is 0.25 porous. Again the dimensionless temperature is low over the porous region (about 0.07) and rises rapidly in the nonporous region reaching a value of 0.66, which happens to be the value obtained on the fully porous plate with half the coolant flow. Thus, to maintain a prescribed maximum surface temperature, the partially porous surfaces will require more total coolant than fully porous surfaces.

CONCLUDING REMARKS

An analysis has been made that determines the effect of upstream surface transpiration cooling on the skin-friction and heat-transfer characteristics of a compressible, laminar boundary layer on a flat plate.

The skin friction has been found to have a low value in the region of transpiration cooling and then to increase until it approaches asymptotically the value for a completely nonporous surface. The initial increase in skin friction is rapid as half of this ultimate increase occurs in a distance beyond the porous region that is only about 20 percent of the length of the porous region for all rates of injection. When the total coolant flow rate is kept constant, however, it is found that the average skin friction on a partially porous plate is even lower than that on a fully porous plate. This occurs because the local transpiration rate per unit area increases for the shorter porous regions so that additional reductions in skin friction in the porous region compensates for the rapid increase in the skin friction over the nonporous region.

Heat-transfer solutions for the nonporous region were obtained for two types of problems: the local heat-transfer rate can be found if the surface temperature distribution is given, and the surface temperature distribution can be found if the local heat-transfer rate is given. A detailed example was presented - the solution to the problem of determining the temperature distribution along the nonporous surface so that there is zero heat transfer at the surface. This corresponds to a thin surface at equilibrium behind a transpiration-cooled region. From this example, it was found that the temperature rises from the value of the transpiration cooled surface and approaches the recovery temperature at large distances along the plate. The initial rise in temperature is quite rapid as half of the ultimate rise in temperature occurs in the region between 1.3 and 2.0 times the porous length, for the range of transpiration coolant rates considered. For constant coolant flow rates, with varying proportions of the porous region length to the total length, it is found that the additional cooling in the porous region due to the higher local coolant flow does not compensate for the rapid rise in temperature over the nonporous region so that the surface temperatures at the end of the plate are larger than would exist on a fully porous plate. For the examples shown, the temperature at the end of the partially porous plate could be maintained at about the same temperature as a fully porous plate by doubling the total rate of coolant flow. In practical application, the increased flow requirements of the partially porous system may be offset somewhat when considerations are made of the weight of the porous surface supporting structure and of thermal radiation from the surface on transient effects which normally cause the rear regions on a surface to have less temperature problems.

Ames Aeronautical Laboratory
National Advisory Committee for Aeronautics
Moffett Field, Calif., March 7, 1957

APPENDIX A

MATHEMATICAL DETAILS OF THE ANALYSIS

Transformation of Basic Equations

Basic equations, assumptions, and boundary conditions.- The basic equations for a compressible, laminar boundary layer with no pressure gradient are:

Continuity equation

$$\frac{\partial}{\partial x'}(\rho' u') + \frac{\partial}{\partial y'}(\rho' v') = 0 \tag{A1}$$

Momentum equation

$$\rho' u' \frac{\partial u'}{\partial x'} + \rho' v' \frac{\partial u'}{\partial y'} = \frac{\partial}{\partial y'}\left(\mu' \frac{\partial u'}{\partial y'}\right) \tag{A2}$$

Energy equation

$$\rho' u' c_p \frac{\partial T'}{\partial x'} + \rho' v' c_p \frac{\partial T'}{\partial y'} = \frac{\partial}{\partial y'}\left(k' \frac{\partial T'}{\partial y'}\right) + \mu'\left(\frac{\partial u'}{\partial y'}\right)^2 \tag{A3}$$

A number of assumptions about the boundary-layer fluid are made to simplify the analysis:

1. $Pr = \frac{c_p \mu'}{k'} = 1$ (A4)

2. c_p = constant

3. The fluid is assumed to behave as a perfect gas, which has an equation of state.

$$p' = \rho' R T' \tag{A5}$$

4. $\frac{\mu'}{\mu_\infty} = C \frac{T'}{T_\infty}$ (A6)

As a result of the first two assumptions, the energy equation (A3) becomes

$$\rho' u' \frac{\partial T'}{\partial x'} + \rho' v' \frac{\partial T'}{\partial y'} = \frac{\partial}{\partial y'}\left(\mu' \frac{\partial T'}{\partial y'}\right) + \frac{\mu'}{c_p}\left(\frac{\partial u'}{\partial y'}\right)^2 \tag{A7}$$

The boundary conditions for the nonporous region, $x' > x_0'$, are

$$\left.\begin{aligned} y' = 0:&\quad u' = 0,\ v' = 0,\ T' = T_s'(x') \\ y' \to \infty:&\quad u' \to u_\infty,\ T' \to T_\infty \end{aligned}\right\} \tag{A8}$$

Stewartson transformation of variables.- The independent variables (x', y') are replaced by a new set of variables (x, y) in which the y' coordinate is modified to take into account the compressibility as done by Stewartson (ref. 5).

$$\left.\begin{aligned} x &= x' \\ y &= \int_0^{y'} \frac{\rho'}{\rho_\infty}\, dy' \end{aligned}\right\} \tag{A9}$$

The formulas relating the derivatives with respect to the physical and transformed independent variables are

$$\left.\begin{aligned} \left(\frac{\partial}{\partial y'}\right)_{x'} &= \frac{\rho'}{\rho_\infty}\left(\frac{\partial}{\partial y}\right)_x \\ \left(\frac{\partial}{\partial x'}\right)_{y'} &= \left(\frac{\partial}{\partial x}\right)_y + \left(\frac{\partial y}{\partial x'}\right)_{y'}\left(\frac{\partial}{\partial y}\right)_x \end{aligned}\right\} \tag{A10}$$

The dependent variables are then related to a stream function ψ, which satisfies the continuity equation and is related to the velocity components as follows:

$$\left.\begin{aligned} \rho' u' &= \rho_\infty \frac{\partial \psi}{\partial y'} \\ \rho' v' &= -\rho_\infty \frac{\partial \psi}{\partial x'} \end{aligned}\right\} \tag{A11}$$

Substitution of equations (A10) and (A11) with the assumptions (A5) and (A6) into equations (A2) and (A7) yields

$$\left(\frac{\partial\psi}{\partial y}\right)\left(\frac{\partial^2\psi}{\partial x\partial y}\right) - \left(\frac{\partial\psi}{\partial x}\right)\left(\frac{\partial^2\psi}{\partial y^2}\right) = C\nu_\infty\left(\frac{\partial^3\psi}{\partial y^3}\right) \tag{A12}$$

$$\left(\frac{\partial\psi}{\partial y}\right)\left(\frac{\partial T'}{\partial x}\right) - \left(\frac{\partial\psi}{\partial x}\right)\left(\frac{\partial T'}{\partial y}\right) = C\nu_\infty\left[\frac{\partial^2 T'}{\partial y^2} + \frac{1}{c_p}\left(\frac{\partial^2\psi}{\partial y^2}\right)^2\right] \tag{A13}$$

To put these equations in the familiar form of the incompressible equations, let u and v be defined by

$$\left.\begin{aligned} u &= \frac{\partial\psi}{\partial y} \\ v &= -\frac{\partial\psi}{\partial x} \end{aligned}\right\} \tag{A14}$$

It is noted from equations (A10) and (A11) that $u = u'$, or that the transformed velocity and the physical velocity components in the x or x' directions are identical. The preceding definition for u and v results in a continuity equation identical to that for an incompressible flow.

$$\frac{\partial u}{\partial x} + \frac{\partial v}{\partial y} = 0 \tag{A15}$$

Substitution of equations (A14) into (A12) and (A13) results in momentum and energy equations identical to those for an incompressible flow.

$$u\frac{\partial u}{\partial x} + v\frac{\partial u}{\partial y} = C\nu_\infty\frac{\partial^2 u}{\partial y^2} \tag{A16}$$

$$u\frac{\partial T}{\partial x} + v\frac{\partial T}{\partial y} = C\nu_\infty\left[\frac{\partial^2 T}{\partial y^2} + \frac{1}{c_p}\left(\frac{\partial u}{\partial y}\right)^2\right] \tag{A17}$$

The primes on the T's are dropped for simplicity. Hence, by use of the Stewartson transformation, the compressible boundary-layer equations have been reduced to equivalent incompressible equations.

In terms of the new coordinates, the boundary conditions (A8) for the nonporous region, $x > x_o$, become

$$\left.\begin{aligned} y = 0: &\quad u = 0,\ v = 0,\ T = T_s(x) \\ y \to \infty: &\quad u \to u_\infty,\ T \to T_\infty \end{aligned}\right\} \tag{A18}$$

Solution of Momentum Equation for Skin Friction

Seventh-degree polynomial velocity profile and evaluation of coefficients.- The boundary-layer velocity profile is approximated by a seventh-degree polynomial in terms of y/δ, where δ is the transformed boundary-layer thickness.

$$\frac{u}{u_\infty} = \sum_{n=1}^{n=7} a_n(x)\left(\frac{y}{\delta}\right)^n \tag{A19}$$

The mth derivative with respect to y is

$$\frac{\partial^{(m)} u}{\partial y^{(m)}} = \frac{u_\infty}{\delta^m}\sum_{n=1}^{n=7} n(n-1).\ .\ .(n-m+1)a_n(x)\left(\frac{y}{\delta}\right)^{n-m} \tag{A20}$$

The slope at the surface is

$$\left(\frac{\partial u}{\partial y}\right)_{y=0} = \frac{a u_\infty}{\delta} \tag{A21}$$

where a is the coefficient of the first power term and is a measure of the shear stress at the surface.

The introduction of the seventh-degree polynomial velocity profile adds seven unknown coefficients to the problem, in addition to the boundary-layer thickness, for a total of eight unknowns. With the momentum integral equation as one equation, seven other equations are required in order to obtain a solution. These equations are obtained by imposing seven conditions on the seventh-degree polynomial velocity profile. Four of the conditions are boundary conditions imposed on the velocity and its derivatives at the outer edge of the boundary layer. To insure that the local velocity in the boundary layer approaches the free-stream velocity smoothly, it is required that for $y = \delta$,

$$\left.\begin{aligned} u &= u_\infty \\ \frac{\partial u}{\partial y} &= \frac{\partial^2 u}{\partial y^2} = \frac{\partial^3 u}{\partial y^3} = 0 \end{aligned}\right\} \tag{A22}$$

Substituting these conditions into equations (A19) and (A20) yields

$$\left.\begin{aligned} a+a_2+a_3+a_4+a_5+a_6+a_7 &= 1 \\ a+2a_2+3a_3+4a_4+5a_5+6a_6+7a_7 &= 0 \\ a_2+3a_3+6a_4+10a_5+15a_6+21a_7 &= 0 \\ a_3+4a_4+10a_5+20a_6+35a_7 &= 0 \end{aligned}\right\} \tag{A23}$$

Before the remaining conditions are imposed, the first and second derivatives with respect to y of the momentum equation (A16) are required. The first derivative is

$$u \frac{\partial^2 u}{\partial x \partial y} + v \frac{\partial^2 u}{\partial y^2} = C\nu_\infty \frac{\partial^3 u}{\partial y^3} \tag{A24}$$

and the second derivative is

$$\frac{\partial u}{\partial y} \frac{\partial^2 u}{\partial x \partial y} + u \frac{\partial^3 u}{\partial x \partial y^2} - \frac{\partial u}{\partial x} \frac{\partial^2 u}{\partial y^2} + v \frac{\partial^3 u}{\partial y^3} = C\nu_\infty \frac{\partial^4 u}{\partial y^4} \tag{A25}$$

The three remaining conditions are imposed at the surface. To insure that the velocity profile has the correct slope and curvature at the surface, the seventh-degree polynomial with the boundary conditions, $u = v = 0$, is substituted into the momentum equation (A16) and its derivatives (A24) and (A25). There results

$$a_2 = a_3 = 0 \tag{A26}$$

and an ordinary differential equation

$$u_\infty \frac{a}{\delta} \frac{d}{dx}\left(u_\infty \frac{a}{\delta}\right) = \frac{24C\nu_\infty u_\infty a_4}{\delta^4} \tag{A27}$$

Equations (A23) and (A26) constitute a system of six algebraic equations with seven unknowns. These equations are solved simultaneously to obtain all the unknowns in terms of the coefficient of the first term, a.

$$\left.\begin{aligned} a_2 &= 0 \\ a_3 &= 0 \\ a_4 &= 35-20a \\ a_5 &= 45a-84 \\ a_6 &= 70-36a \\ a_7 &= 10a-20 \end{aligned}\right\} \qquad \text{(A28)}$$

Substituting a_4 from equation (A28) into equation (A27) and carrying out the differentiation yields

$$\frac{u_\infty a\delta}{C\nu_\infty}\left(\delta\frac{da}{dx} - a\frac{d\delta}{dx}\right) = (35-20a)24 \qquad \text{(A29)}$$

This equation, in part, determines how the slope of the velocity profile at the surface varies with the distance along the surface.

Momentum integral equation.- The momentum integral equation is obtained by integrating the momentum equation (A16) from $y = 0$ to $y = \delta$.

$$\frac{C\nu_\infty}{u_\infty^2}\left(\frac{\partial u}{\partial y}\right)_{y=0} = \frac{\partial}{\partial x}\int_0^\delta \frac{u}{u_\infty}\left(1-\frac{u}{u_\infty}\right)dy \qquad \text{(A30)}$$

The assumed velocity profile (A19) with the coefficients expressed in terms of a from equations (A28) and the slope at the surface given by equation (A21) are substituted into equation (A30). The integration is carried out to yield

$$\frac{C\nu_\infty a}{u_\infty\delta} = \frac{d}{dx}\left[\delta(A_1+A_2a-A_3a^2)\right] \qquad \text{(A31)}$$

where

$$\left.\begin{aligned} A_1 &= 0.09518 \\ A_2 &= 0.04371 \\ A_3 &= 0.01832 \end{aligned}\right\} \qquad \text{(A32)}$$

Reduction of problem to solution of two simultaneous ordinary differential equations.- Equations (A29) and (A31) form a system of two simultaneous ordinary differential equations in a, δ, and x. These equations can be simplified by expressing δ and x in terms of Reynolds numbers.

$$\left.\begin{aligned} R_\delta &= \frac{\delta u_\infty}{C\nu_\infty} \\ R_x &= \frac{x u_\infty}{C\nu_\infty} \end{aligned}\right\} \tag{A33}$$

Substituting these Reynolds numbers into equations (A29) and (A31) yields

$$R_\delta a\left(R_\delta \frac{da}{dR_x} - a\frac{dR_\delta}{dR_x}\right) = 24(35-20a) \tag{A34}$$

$$\frac{a}{R_\delta} = \frac{d}{dR_x}\left[R_\delta\left(A_1+A_2a-A_3a^2\right)\right] \tag{A35}$$

The preceding equations can be manipulated to separate the derivatives and yield

$$\frac{dR_\delta}{dR_x} = \frac{\alpha_1(a)}{R_\delta} \tag{A36}$$

$$\frac{da}{dR_x} = \frac{\alpha_2(a)}{R_\delta^2} \tag{A37}$$

where

$$\left.\begin{aligned} \alpha_1(a) &= \frac{120}{a}\left[\frac{-7A_2+(4A_2+14A_3)a+\left(\frac{1}{120}-8A_3\right)a^2}{A_1+2A_2a-3A_3a^2}\right] \\ \alpha_2(a) &= \frac{120}{a}\left[\frac{7A_1+(7A_2-4A_1)a-(4A_2+7A_3)a^2+\left(\frac{1}{120}+4A_3\right)a^3}{A_1+2A_2a-3A_3a^2}\right] \end{aligned}\right\} \tag{A38}$$

The Reynolds numbers R_δ and R_x can be normalized by substituting

$$\left.\begin{aligned} \xi &= \frac{R_x}{R_{x_o}} = \frac{x}{x_o} \\ \delta^+ &= \frac{R_\delta}{R_{\delta_o}} = \frac{\delta}{\delta_o} \\ D_o &= \frac{{R_{\delta_o}}^2}{R_{x_o}} \end{aligned}\right\} \tag{A39}$$

Equations (A36) and (A37) then become

$$\frac{d\delta^+}{d\xi} = \frac{\alpha_1(a)}{D_o\delta^+} \tag{A40}$$

$$\frac{da}{d\xi} = \frac{\alpha_2(a)}{D_o(\delta^+)^2} \tag{A41}$$

The initial conditions at this stage are

$$\xi = 1,\ \delta^+ = 1 \tag{A42}$$

Before the equations can be solved, it is necessary to know the initial conditions for a and D_o.

Determination of initial conditions for solution of momentum equation.- Before a solution can be obtained for equations (A40) and (A41), it is necessary to obtain the initial conditions for a and D_o by matching the seventh-degree polynomial, both in thickness and slope at the surface, to the exact profile at the end of the transpiration-cooled region. Since the seventh-degree polynomial profile assumes a finite boundary-layer thickness, whereas in the exact profile the velocity approaches the free-stream velocity asymptotically, a problem arises in defining the outer edge of the boundary layer. In this analysis the no transpiration or Blasius case is used to make this definition.

For the Blasius case, the shear stress at the surface, or the skin-friction coefficient, varies as $R_x^{-1/2}$, and the boundary-layer thickness varies as $R_x^{1/2}$. The product of the two quantities is, therefore, independent of R_x. For the present solution, the product of the shear stress at the surface, which is proportional to the slope at the surface as given in equation (A21), and the boundary-layer thickness is a function of a alone. For a to be independent of R_x, it follows from equation (A37) that $\alpha_2(a) = 0$ or $a_B = 1.871$. This value of a_B for the seventh-degree polynomial with no transpiration cooling must now be related to the exact solution.

The following relations for the exact solution are obtained from reference 2.

$$R_\delta = 2\sqrt{R_x}\,\eta_\delta \tag{A43}$$

$$\frac{c_f}{2} = \frac{1}{4}\frac{f''(0)}{\sqrt{R_x}} \tag{A44}$$

$$\frac{u}{u_\infty} = \frac{1}{2}f'(\eta_\delta) \tag{A45}$$

The function $f(\eta)$ is a dimensionless stream function, and η is the similarity variable with η_δ denoting its value at the outer edge of the boundary layer.

The local skin-friction coefficient is defined as

$$\frac{c_f}{2} = \frac{\tau_s'}{\rho_\infty u_\infty^2} \tag{A46}$$

where

$$\tau_s' = \mu'_s\left(\frac{\partial u'}{\partial y'}\right)_{y=0} \tag{A47}$$

For the present analysis, the local skin-friction coefficient is obtained by substituting equations (A5), (A6), (A10), (A21), and (A47) into equation (A46). There results

$$\frac{c_f}{2} = \frac{a}{R_\delta} \tag{A48}$$

The boundary-layer thickness and the local skin-friction coefficient, which is determined by the slope of the velocity profile at the surface, for the seventh-degree polynomial solution and the exact transpiration cooling solution are now equated. From equations (A43), (A44), and (A48) there results

$$\eta_\delta = \frac{2a}{f''(0)} \tag{A49}$$

With no transpiration cooling, $a_B = 1.871$, $f''(0) = 1.3282$, and $\eta_\delta = 2.818$. From table II of reference 2 and the relation (A45), the outer edge of the boundary layer is defined as the point where the velocity ratio is

$$\frac{u}{u_\infty} = \frac{1}{2} f'(\eta_\delta) = 0.9976 \tag{A50}$$

This definition is used to define the boundary-layer thickness when transpiration cooling occurs.

The initial conditions for the solution of equations (A40) and (A41) are thus determined as follows: A value of $f(0)$ is selected using equation (5), the absolute magnitude of $f(0)$ being proportional to the amount of transpiration cooling. With the outer edge of the boundary layer defined by equation (A50), the value of η_δ is determined from table II, reference 2. Then a is calculated from equation (A49), and D_o is calculated from equation (A43). With these initial conditions, the system of two simultaneous ordinary differential equations (A40) and (A41) was integrated numerically on an IBM 650 computing machine to obtain a and δ^+ as functions of ξ for $\xi = 1$ to $\xi = 10$. Five different transpiration cooling rates were selected, including the Blasius case. The results are expressed in terms of the local skin-friction coefficient as given by equation (A48).

Solution of Energy Equation

Separation of solutions.- Because the surface temperature of the nonporous region will normally differ from the constant surface temperature of the transpiration-cooled region, it is necessary in this analysis to obtain a solution of the energy equation (A17) that accounts for surface temperature variations. The method of solution followed will be to obtain a solution for the complete inhomogeneous energy equation when the porous and nonporous regions are at the same temperature. Then solutions of the homogeneous portion of the energy equation are added to satisfy the surface temperature boundary conditions. This addition of solutions is permissible because the energy equation is linear in temperature.

Solution of inhomogeneous energy equation.- The inhomogeneous energy equation (A17) is solved for the case of a constant surface temperature, T_c. If the momentum equation (A16) is multiplied by u/c_p and added to the energy equation (A17), there results

$$u \frac{\partial}{\partial x}\left(T + \frac{u^2}{2c_p}\right) + v \frac{\partial}{\partial y}\left(T + \frac{u^2}{2c_p}\right) = C\nu_\infty\left[\frac{\partial^2}{\partial y^2}\left(T + \frac{u^2}{2c_p}\right)\right] \tag{A51}$$

Because this equation has the same form as the momentum equation, if u is a solution of the momentum equation, then

$$T + \frac{u^2}{2c_p} = C_1 u + C_2 \tag{A52}$$

must be a solution of the energy equation. When the boundary conditions,

$$\left.\begin{aligned} u &= 0, \; T = T_c \\ u &= u_\infty, \; T = T_\infty \end{aligned}\right\} \tag{A53}$$

are imposed, the unknown constants,

$$\left.\begin{aligned} C_1 &= \frac{T_t - T_c}{u_\infty} \\ C_2 &= T_c \end{aligned}\right\} \tag{A54}$$

are determined. Hence, an exact solution of the energy equation for the case of a constant surface temperature is

$$T_I = (T_t - T_c)\frac{u}{u_\infty} + T_c - \frac{u^2}{2c_p} \tag{A55}$$

Solution of homogeneous energy equation for single discontinuity in surface temperature.- The homogeneous energy equation is solved for a single discontinuity in surface temperature. The boundary conditions on the surface temperature are for

$$\left.\begin{aligned} x \leq x_j \,, \quad & T = T_\infty \\ x > x_j \,, \quad & T = T_s \end{aligned}\right\} \tag{A56}$$

where $x_j \geq x_o$ is the location of a surface temperature discontinuity.

In order to obtain a solution of the homogeneous portion of the energy equation, which is equation (A17) with the viscous dissipation term neglected, the boundary-layer velocity profile is assumed linear with the correct slope at the surface, as determined previously in the solution of the momentum equation. The x component of velocity is assumed to be

$$u = s(x)y = \left(\frac{\partial u}{\partial y}\right)_{y=o} y \tag{A57}$$

The y component of velocity is obtained by integrating the continuity equation (A15) with respect to y.

$$v = -\int_0^y \frac{\partial u}{\partial x}\, dy = -\frac{1}{2}\left(\frac{ds}{dx}\right)y^2 \tag{A58}$$

The temperature distribution in the boundary layer is assumed to be a function of a single parameter ζ, where

$$\frac{T-T_s}{T_\infty - T_s} = \theta(\zeta) \tag{A59}$$

and

$$\zeta = X(x)Y(x, x_j)y \tag{A60}$$

where X and Y are two arbitrary functions of x and x_j. From equations (A56), (A59), and (A60), the boundary conditions on θ are

$$\left.\begin{aligned} x \leq x_j:&\quad \text{all } y, \quad \theta = 1 \\ \text{all } x:&\quad y \to \infty, \quad \theta = 1 \\ x > x_j:&\quad y = 0, \quad \theta = 0 \end{aligned}\right\} \tag{A61}$$

Substitution of equations (A57), (A58), (A59), and (A60) into the homogeneous portion of the energy equation (A17) yields

$$\frac{s}{X^3Y^3}\left(\frac{1}{X}\frac{dX}{dx} + \frac{1}{Y}\frac{dY}{dx} - \frac{1}{2s}\frac{ds}{dx}\right) = \frac{C\nu_\infty}{\zeta^2}\frac{d^2\theta/d\zeta^2}{d\theta/d\zeta} \tag{A62}$$

If ζ and x are independent variables, both sides of equation (A62) must equal a constant, say $-C\nu_\infty$

$$\frac{s}{X^3Y^3}\left(\frac{1}{X}\frac{dX}{dx} + \frac{1}{Y}\frac{dY}{dx} - \frac{1}{2s}\frac{ds}{dx}\right) = -C\nu_\infty \tag{A63}$$

$$\frac{d^2\theta}{d\zeta^2} + \zeta^2\frac{d\theta}{d\zeta} = 0 \tag{A64}$$

Since X is an arbitrary function of x, let

$$\frac{1}{X}\frac{dX}{dx} - \frac{1}{2s}\frac{ds}{dx} = 0 \tag{A65}$$

Upon integration,

$$X = C_3 s^{1/2} \tag{A66}$$

Substituting equation (A66) into (A63), there results

$$\frac{1}{Y^4}\frac{dY}{dx} = -C\nu_\infty C_3{}^3 s^{1/2} \tag{A67}$$

Upon integration with the boundary condition, $x = x_j$, $Y \rightarrow \infty$, the arbitrary function Y is determined as

$$Y = \frac{1}{C_3\left(3C\nu_\infty \int_{x_j}^{x} s^{1/2} dx\right)^{1/3}} \tag{A68}$$

The variable ζ is from equations (A60), (A66), and (A68),

$$\zeta = XYy = \frac{s^{1/2} y}{\left(3C\nu_\infty \int_{x_j}^{x} s^{1/2} dx\right)^{1/3}} \tag{A69}$$

The function θ is found by integrating equation (A64) with the boundary condition $\theta(0) = 0$.

$$\theta = C_4 \int_0^{\zeta} e^{-\zeta^3/3} d\zeta \tag{A70}$$

The constant C_4 is determined from the boundary condition, $\theta(\infty) = 1$.

$$C_4 = \frac{1}{\int_0^\infty e^{-\zeta^3/3} d\zeta} = \frac{1}{3^{1/3}\Gamma\left(\frac{4}{3}\right)} \tag{A71}$$

The complete solution of the homogeneous equation for the boundary conditions (A61) is

$$\theta(\zeta) = \frac{T-T_s}{T_\infty - T_s} = \frac{1}{3^{1/3}\Gamma\left(\frac{4}{3}\right)} \int_0^\zeta e^{-\zeta^3/3} d\zeta \tag{A72}$$

General solution of energy equation.- Addition of solutions (A55) and (A72) with $x_j = x_o$ yields the temperature distribution in the boundary layer of a flat plate with the porous surface at a constant temperature T_c and the nonporous surface at a different constant temperature T_s. In order to obtain the solution when the temperature of the nonporous surface is arbitrary, homogeneous solutions of the form (A72) can be added as shown in reference 6, because the energy equation is linear in temperature. For r surface temperature discontinuities in the nonporous region, $x > x_o$, the temperature is given by

$$T(x,y) = T_I - T_c + \sum_{j=1}^{j=r-1} (T_{s_j} - T_{s_{j+1}})\theta(x,y,x_j) + T_{s_r} \tag{A73}$$

where

$$T_{s_1} = T_c$$

As $r \to \infty$, the summation approaches an integral such that

$$T(x,y) = T_I - T_c + T_s(x) - \int_{x_o}^{x} \frac{dT_s(x_1)}{dx_1} \theta(x,y,x_1) dx_1 \tag{A74}$$

The general solution of the energy equation for an arbitrary surface temperature distribution in the nonporous region is then

$$T(x,y) = T_s(x) + (T_t - T_c) \frac{u}{u_\infty} - \frac{u^2}{2c_p} - \int_{x_o}^{x} \frac{dT_s(x_1)}{dx_1} \theta(x,y,x_1) dx_1 \tag{A75}$$

It should be noted from equations (A9) and (A10) that

$$\frac{dT_s}{dx} = \frac{dT_s'}{dx'} \tag{A76}$$

Heat transfer at the surface.- The heat transfer at the surface per unit area is by definition and from equation (A10)

$$q_s = -k_s\left(\frac{\partial T'}{\partial y'}\right)_{y'=0} = -Ck_\infty\left(\frac{\partial T}{\partial y}\right)_{y=0} \tag{A77}$$

Substitution of equation (A75) into (A77) yields

$$q_s = -\frac{Ck_\infty}{u_\infty}(T_t-T_c)\left(\frac{\partial u}{\partial y}\right)_{y=0} + Ck_\infty\int_{x_0}^{x}\frac{dT_s(x_1)}{dx_1}\left(\frac{d\theta}{d\zeta}\right)_{y=0}\left(\frac{d\zeta}{dy}\right)_{y=0}dx_1 \tag{A78}$$

From equation (A69)

$$\left(\frac{\partial\zeta}{\partial y}\right)_{y=0} = \frac{s^{1/2}}{\left(3C\nu_\infty\int_{x_0}^{x}s^{1/2}dx\right)^{1/3}} \tag{A79}$$

From equation (A72)

$$\left(\frac{d\theta}{d\zeta}\right)_{y=0} = \frac{1}{3^{1/3}\Gamma\left(\frac{4}{3}\right)} \tag{A80}$$

Substituting equations (A79) and (A80) into (A78) results in the equation for the heat transfer at the surface for a given surface temperature distribution.

$$q_s(x) = -\frac{Ck_\infty(T_t-T_c)s}{u_\infty} + \left(\frac{3C^2}{\nu_\infty}\right)^{1/3}\frac{k_\infty s^{1/2}}{\Gamma\left(\frac{1}{3}\right)}\int_{x_0}^{x}\frac{\frac{dT_s(x_1)}{dx_1}}{\left(\int_{x_1}^{x}s^{1/2}dx_2\right)^{1/3}}dx_1 \tag{A81}$$

The variables are normalized by letting

$$\left.\begin{aligned} \xi &= \frac{x}{x_o} \\ \delta^+ &= \frac{\delta}{\delta_o} \end{aligned}\right\} \tag{A82}$$

Also, the following substitutions are made

$$\left.\begin{aligned} \sigma(\xi) &= \frac{a}{\delta^+} = \frac{\delta_o}{u_\infty} s(x) \\ \varphi(\xi) &= \int_1^\xi \sqrt{\sigma(\xi)}\, d\xi \end{aligned}\right\} \tag{A83}$$

Then, the heat transfer at the surface, equation (A81), in terms of the normalized variables becomes

$$q_s(\xi) = -\frac{\rho_\infty u_\infty c_p}{R_{\delta_o}} \sqrt{\sigma(\xi)} \left[(T_t - T_c)\sqrt{\sigma(\xi)} - 0.538 D_o^{1/3} \int_1^\xi \frac{\frac{dT_s(\xi_1)}{d\xi_1}}{[\varphi(\xi) - \varphi(\xi_1)]^{1/3}} d\xi_1 \right] \tag{A84}$$

<u>Surface temperature with prescribed heat transfer at the surface</u>.- With the heat transfer at the surface prescribed, the surface temperature is given by the following integral equation based on equation (A84).

$$\int_1^\xi \frac{\frac{dT_s(\xi_1)}{d\xi_1}}{[\varphi(\xi) - \varphi(\xi_1)]^{1/3}} d\xi_1 = \Omega(\xi) \tag{A85}$$

where

$$\Omega(\xi) = \frac{1.858}{D_o^{1/3}} \left[\frac{R_{\delta_o} q_s(\xi)}{\rho_\infty u_\infty c_p \sqrt{\sigma(\xi)}} + (T_t - T_c)\sqrt{\sigma(\xi)} \right] \tag{A86}$$

The independent variable is now changed from ξ to φ in equation (A85) to yield

$$\int_0^{\varphi} \frac{\frac{dT_s(\varphi_1)}{d\varphi_1}}{(\varphi-\varphi_1)^{1/3}}\, d\varphi_1 = \Omega(\varphi) \tag{A87}$$

The integral equation now has the same form as Volterra's equation of the first kind with the kernel becoming infinite at the upper limit. Solution of this equation is given in reference 7.

$$\frac{dT_s(\varphi)}{d\varphi} = \frac{\sin\,(\pi/3)}{\pi}\, \frac{d}{d\varphi}\left[\int_0^{\varphi} \frac{\Omega(\varphi_1)d\varphi_1}{(\varphi-\varphi_1)^{2/3}}\right] \tag{A88}$$

Upon integration from $\varphi = 0$ to φ,

$$T_s(\varphi) = \frac{\sin\,(\pi/3)}{\pi} \int_0^{\varphi} \frac{\Omega(\varphi_1)d\varphi_1}{(\varphi-\varphi_1)^{2/3}} \tag{A89}$$

Now the independent variable is changed back to ξ

$$T_s(\xi)-T_c = \frac{\sin\,(\pi/3)}{\pi} \int_1^{\xi} \frac{\Omega(\xi_1)\sqrt{\sigma(\xi_1)}\, d\xi_1}{[\varphi(\xi)-\varphi(\xi_1)]^{2/3}} \tag{A90}$$

Consider the special case where the nonporous surface is insulated or $q_s(\xi) = 0$ in equation (A86). Then

$$\Omega(\xi) = \frac{\Gamma\left(\frac{1}{3}\right)}{(3D_o)^{1/3}}\, (T_t-T_c)\sqrt{\sigma(\xi)} \tag{A91}$$

The temperature of the insulated surface is then

$$\frac{T_s(\xi)-T_c}{T_t-T_c} = \frac{0.512}{D_o^{1/3}} \int_1^{\xi} \frac{\sigma(\xi_1)d\xi_1}{[\varphi(\xi)-\varphi(\xi_1)]^{2/3}} \tag{A92}$$

Solution of equation (A92) was performed on an IBM 650 computing machine.

REFERENCES

1. Eckert, E. R. G., and Livingood, John N. B.: Comparison of Effectiveness of Convection-, Transpiration, and Film-Cooling Methods With Air as Coolant. NACA TN 3010, 1953.

2. Low, George M.: The Compressible Laminar Boundary Layer With Fluid Injection. NACA TN 3404, 1955.

3. Emmons, H. W., and Leigh, D.: Tabulation of the Blasius Function With Blowing and Suction. Interim Tech. Rep. No. 9, Harvard University, Combustion Aerodynamics Lab., Nov. 1953.

4. Lew, H. G., and Fanucci, J. B.: An Exact Solution of the Laminar Boundary Layer With Zero Pressure Gradient and Homogeneous Injection. Tech. Rep. No. 6, Penn. State Univ., Dept. of Aero. Eng., July 1955.

5. Stewartson, K.: Correlated Incompressible and Compressible Boundary Layers. Proc. Roy. Soc. (London), ser. A, vol. 200, no. 1060, Dec. 22, 1949, pp. 84-100.

6. Rubesin, Morris W.: The Effect of an Arbitrary Surface-Temperature Variation Along a Flat Plate on the Convective Heat Transfer in an Incompressible Turbulent Boundary Layer. NACA TN 2345, 1951.

7. Margenau, Henry, and Murphy, George Moseley: The Mathematics of Physics and Chemistry. D. Van Nostrand Company, Inc., N. Y., 1943, pp. 506-507.

TABLE I.- EFFECT OF UPSTREAM TRANSPIRATION COOLING RATES ON INITIAL CONDITIONS FOR PRESENT ANALYSIS

$F=f(0)$	D_o	$\sigma(1)$
0	31.76	1.871
-.25	37.77	1.504
-.50	45.97	1.115
-.75	58.83	.718
-1.00	83.87	.325

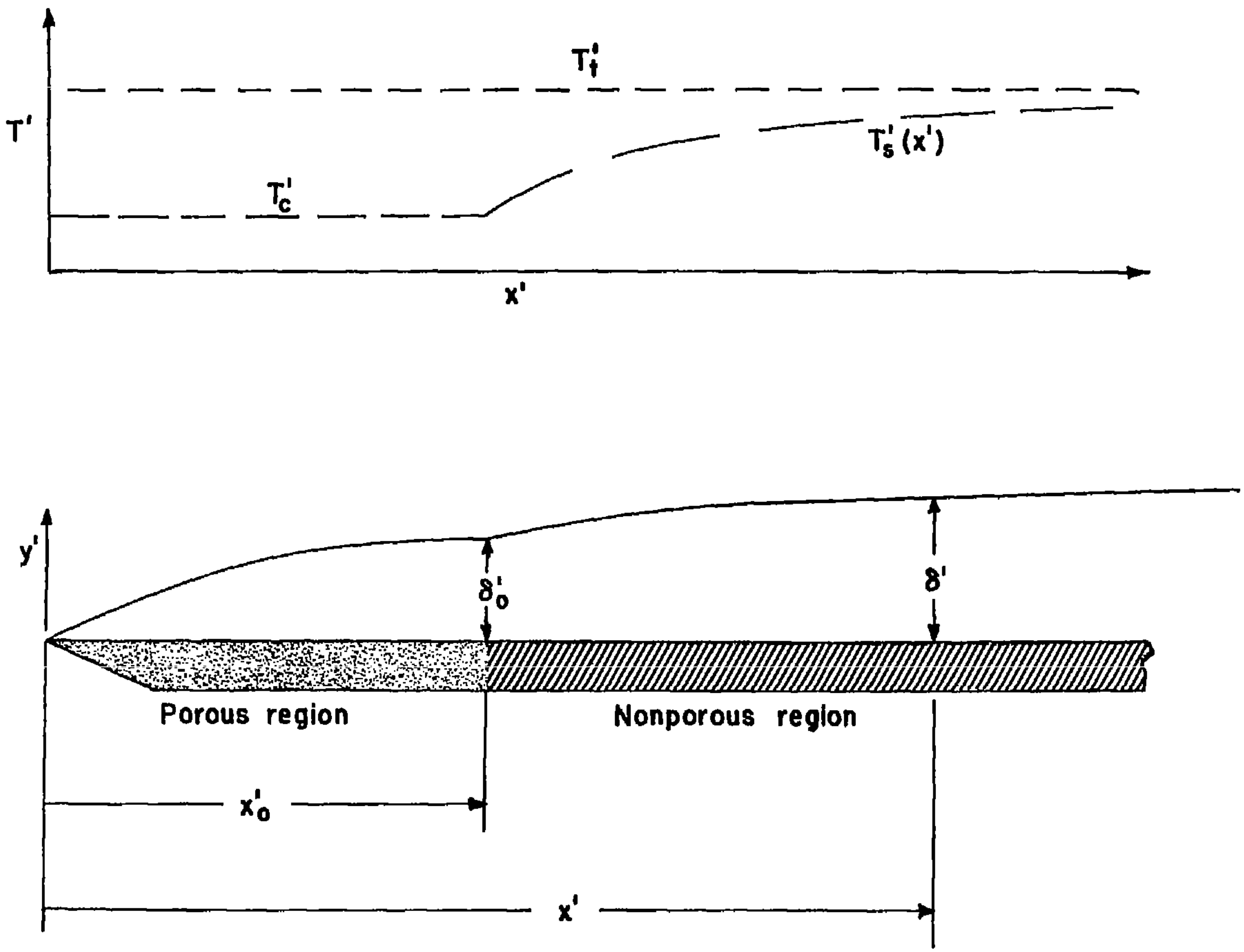

Figure 1.- Sketch of boundary layer on a flat plate with upstream transpiration cooling.

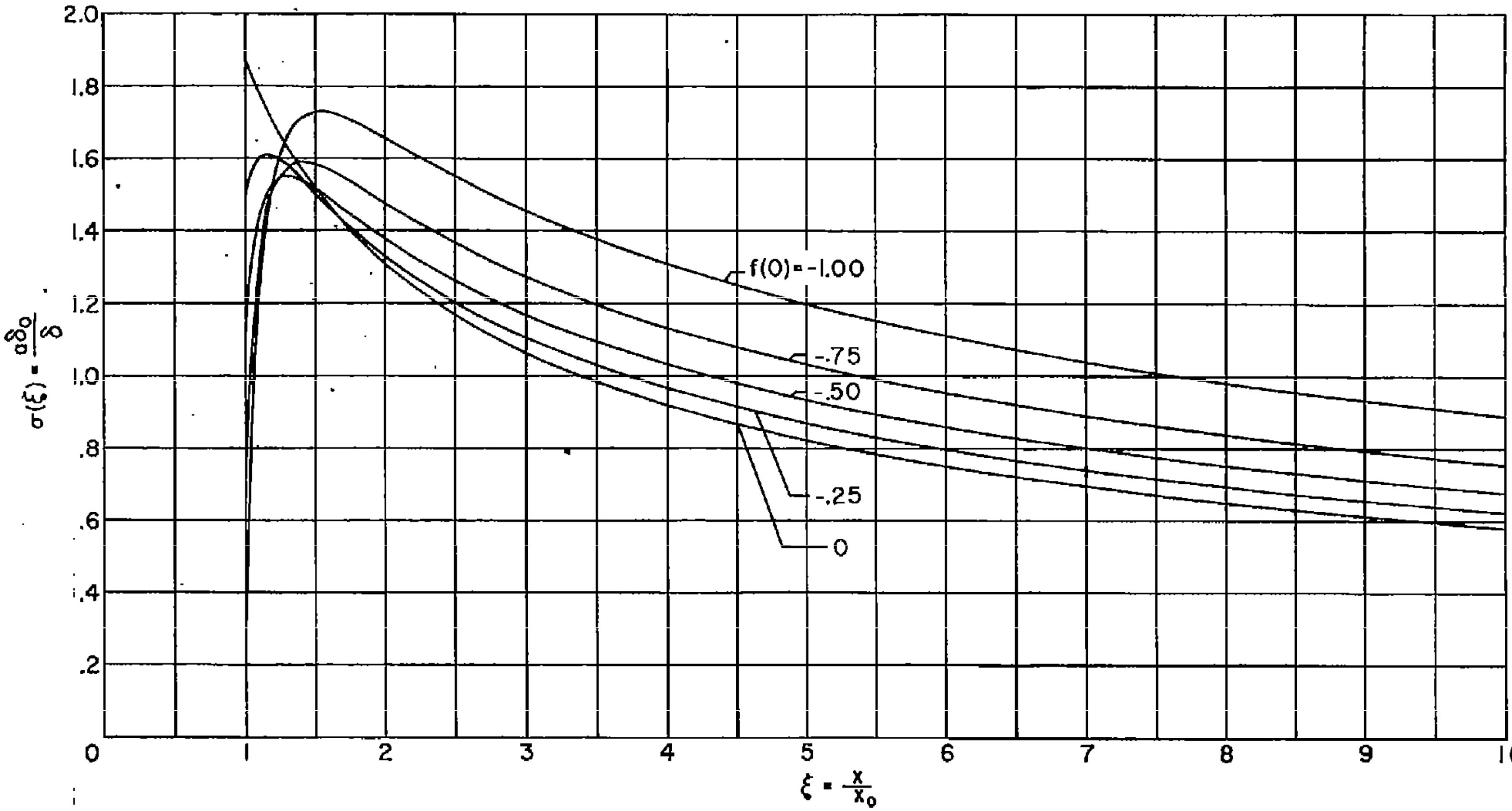

Figure 2.- Distribution of dimensionless shear function along plate.

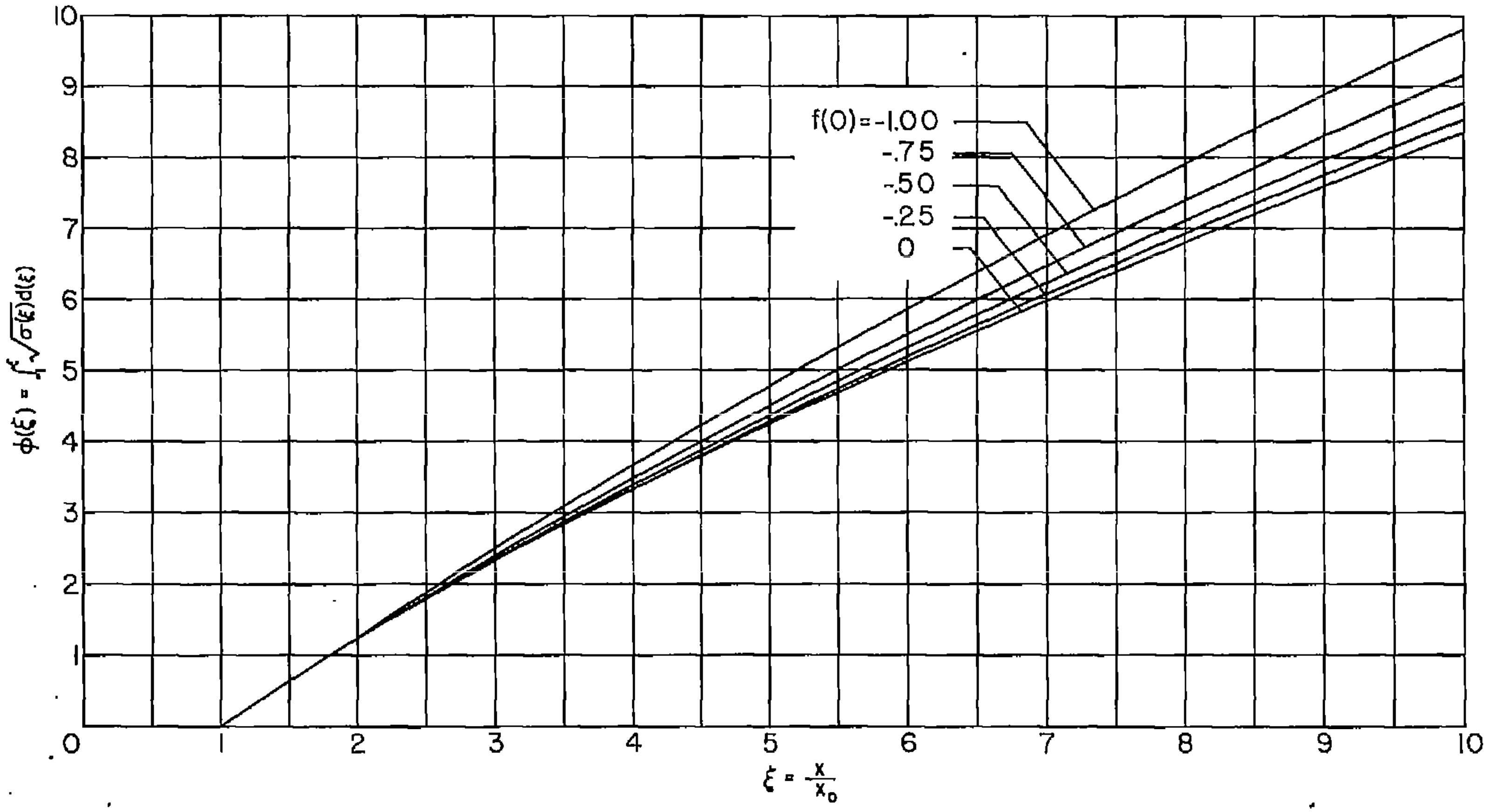

Figure 3.- Integral of dimensionless shear function along plate.

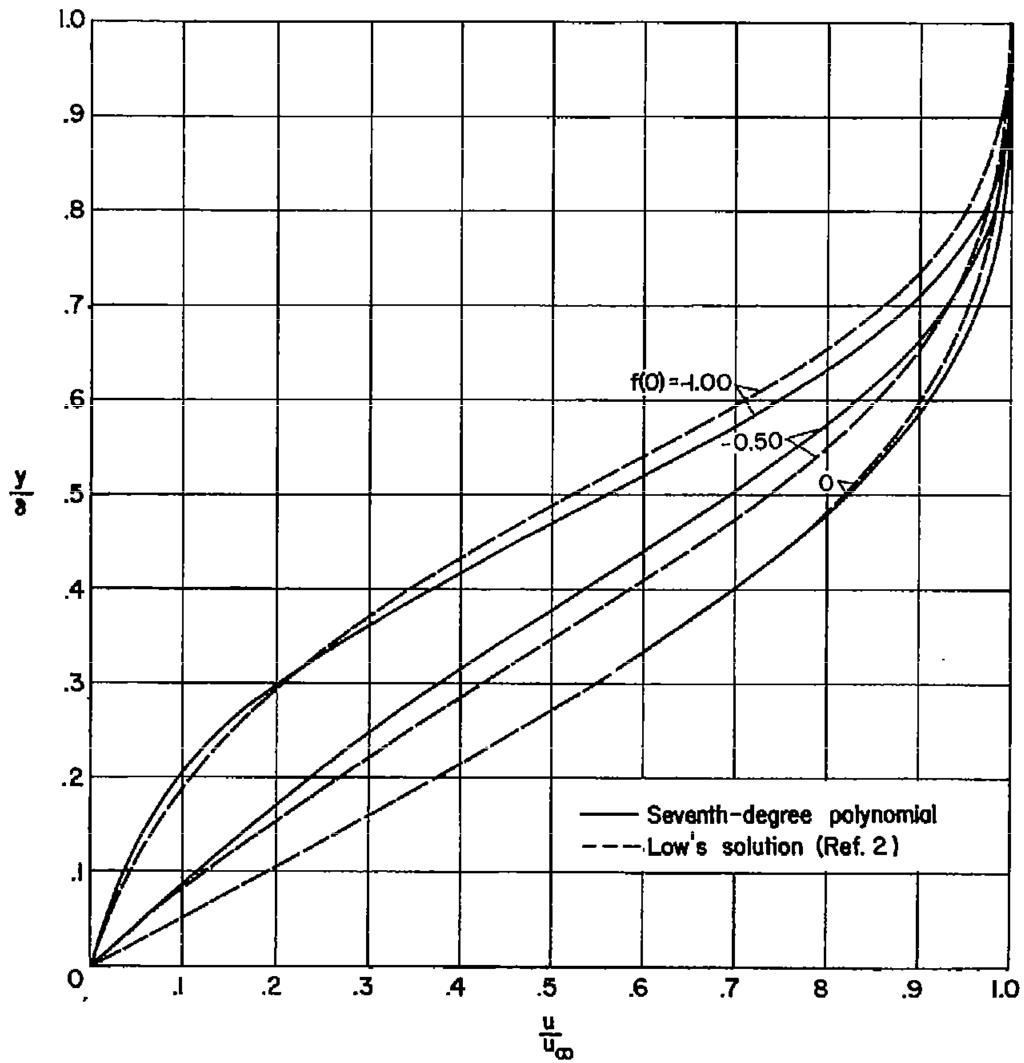

Figure 4.- Comparison of seventh-degree polynomial velocity profile with Low's exact solution for various transpiration cooling rates.

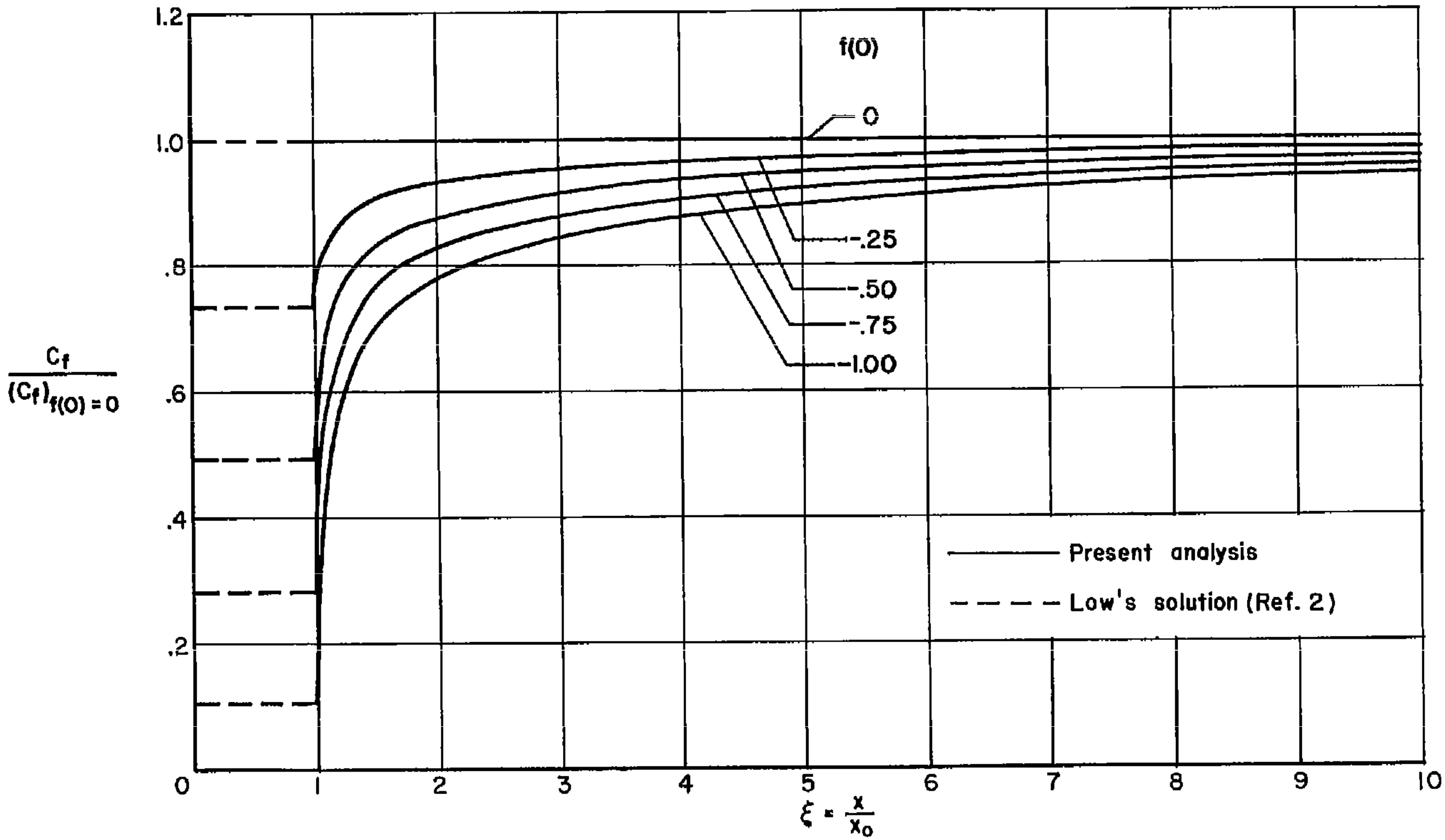

Figure 5.- Local skin friction on a flat plate with upstream surface transpiration cooling.

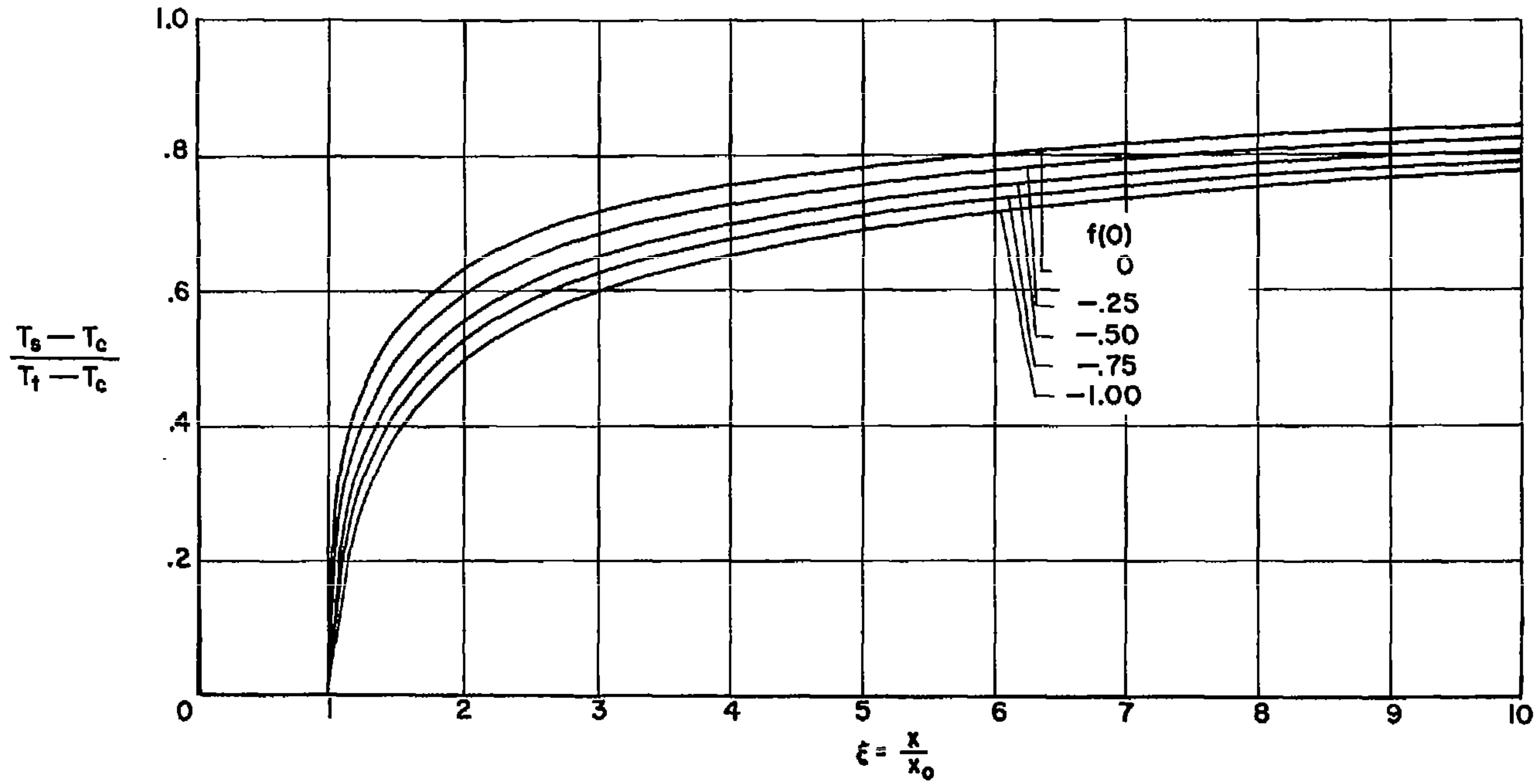

Figure 6.- Temperature distribution on an insulated nonporous plate behind a region with transpiration cooling.

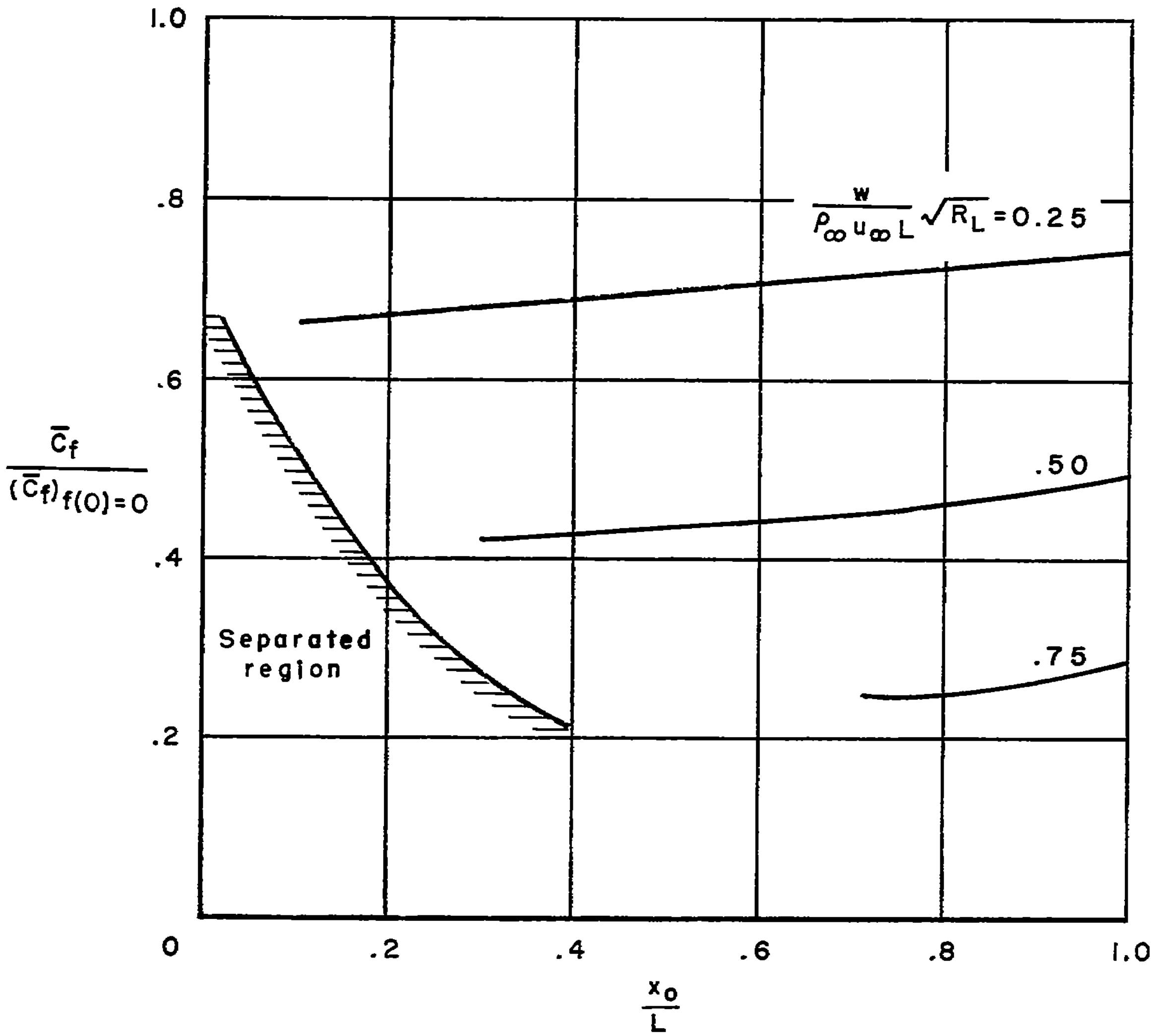

Figure 7.- The effect on the average skin friction of varying the porous length of a partially transpiration-cooled plate subject to constant total coolant rate.

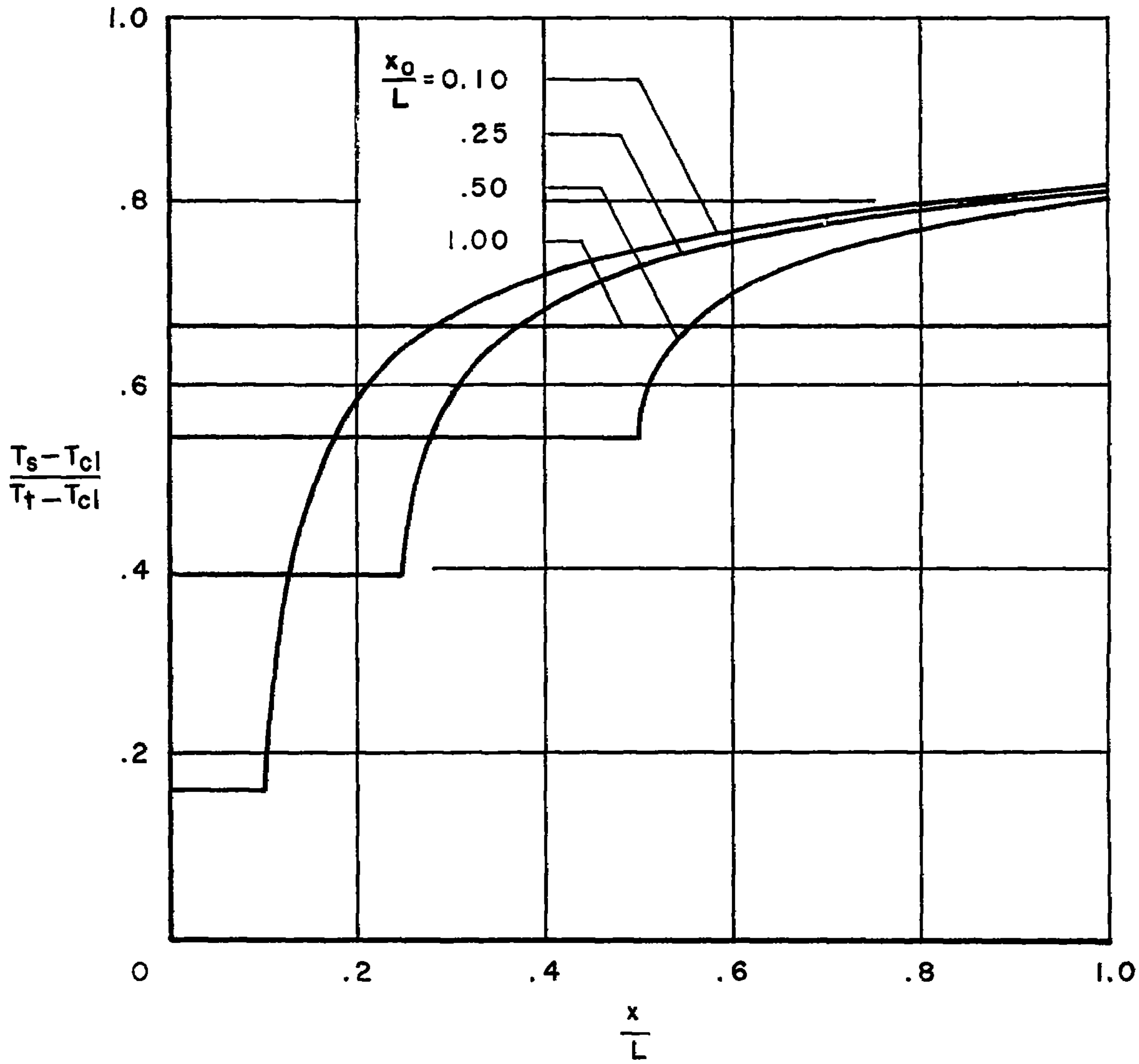

(a) $\frac{w}{\rho_\infty u_\infty L}\sqrt{R_L} = 0.25$

Figure 8.- The effect on the temperature distribution of varying the porous length of a partially transpiration-cooled plate subject to constant total coolant flow at a fixed temperature.

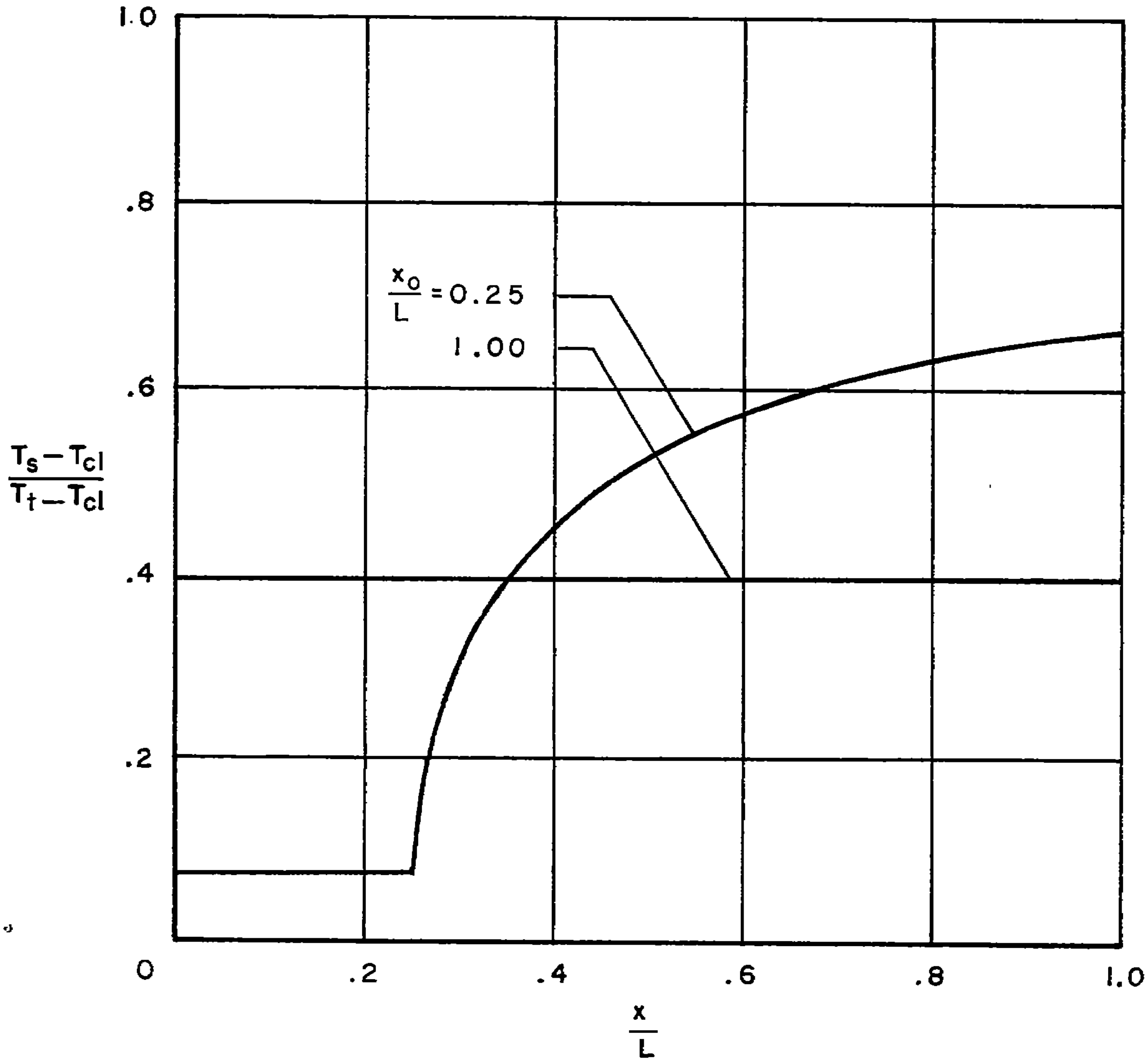

(b) $\frac{w}{\rho_\infty u_\infty L}\sqrt{R_L} = 0.50$

Figure 8.- Concluded.

NACA - Langley Field, Va.